10. The data we report were obtained from the following typical experimental procedures. All data has been shown to be reproducible with an error of ~5%. The oxidation of methane was conducted in a 300-ml high-pressure, stirred autoclave from Autoclave Engineers. The reactor was modified so that all the internal parts were either glass-lined or made from tantalum. The reactor was equipped with baffles, a hollow shaft/impeller, and was stirred at 1500 rpm to insure thorough gas-liquid mixing during the reaction. The reactor was loaded with the Pt catalyst (typically 20 to 50 mM) along with 80 to 120 ml H_2SO_4 (at desired concentration), and the system was degassed with N. The reactor was heated to the desired reaction temperature (typically between 180° and 220°C), and a mixture of 97% methane and 3% neon was added to a total pressure of 500 psig. The methane/neon feed was added to the reactor from a known-volume reservoir in which the temperature and pressure of the gas was measured before and after addition so that the total moles of methane/neon added to the reactor could be accurately determined. The reaction was typically allowed to proceed for 1 to 3 hours. Cooling to near room temperature with an external, water-cooled line stopped the reaction, and the gas phase was vented into a 20-liter pressure vessel. After allowing several hours for thorough gas mixing, the vented gas was analyzed with a Hewlett-Packard 5880 GC equipped with a Hayesep D column and a thermal conductivity detector. The molar composition in the vented gas (primarily CH_4, CO_2, SO_2, and CH_3Cl) was determined on the basis of the reference neon internal standard; molar ratios of the gases; and the temperature, pressures, and volume of the vented gas. The liquid phase remaining in the 300-ml high-pressure reactor was analyzed by ^1H and ^{13}C NMR and high-pressure liquid chromatography (HPLC) analyses. For NMR analysis, a known amount of acetic acid was added to an aliquot of the reaction solution as an internal standard. Methyl bisulfate (and any free methanol) was determined from the ratio of the ^1H NMR methyl resonances of methyl bisulfate (3.4 ppm) to acetic acid (2.02 ppm). The methyl products were also quantified by HPLC analysis of the liquid phase. Known volume aliquots of reaction solution were first hydrolyzed by the addition of three parts water to one part crude reaction solution and heated to 90°C for 4 hours in a sealed vial. The hydrolyzed solution was analyzed with a Hewlett-Packard 1050 HPLC equipped with an HPX-87H column (Bio-Rad) and a refractive index detector. The eluent was 0.1 volume % H_2SO_4 in water. Methanol eluted at 16.2 min. The gas phase (CH_4, CO_2 and CH_3Cl) and liquid phase (CH_3OSO_3H and CH_3OH) analyses allowed >90 to 95% mass balance on methane.
11. Oxidation of the Pt(II) center to Pt(IV) occurs as evidenced by changes in the solution NMR spectra. Free ligand is generated, but no reaction at the C–H bonds is observed.
12. Calculated volumetric productivity based on the liquid phase for this reaction is $\sim 10^{-7}$ mol ml^{-1} s^{-1}; Catalyst turnover number (~20) and catalyst TOF ($\sim 10^{-3}$ s^{-1}) were values obtained over the integrated reaction time.
13. The catalyst was still active after 500 turnovers. The reaction was stopped at this point. The actual number of turnovers before the regeneration would be required has not been determined.
14. The exact value depends on the value for the solubility of methane in H_2SO_4 used in the calculations.
15. M. W. Holtcamp, J. A. Labinger, J. E. Bercaw, *J. Am. Chem. Soc.* **119**, 848 (1997) and references therein.
16. At temperatures below 150°C, negligible methane oxidation (<1%) is observed with concentrated H_2SO_4 containing **1** under typical reaction conditions over a 30-min period.
17. Assuming the microscopic reverse of the C–H activation step, protonolysis of the methyl Pt bond is significantly more rapid than the C–H activation step.
18. The lack of any redox change in the Pt center is evidenced by the stability of the (bpym)PtX_2 complex, absence of reduced Pt, lack of methyl bisulfate or overoxidation products such as CO_2, and lack of reduction products such as SO_2.
19. If H/D exchange is occurring with these oxidation states the rates must be at least three orders of magnitude slower than with Pt(II).
20. C. Hall and R. N. Perutz, *Chem. Rev.* **96**, 3125 (1996); J. J. Schneider, *Angew. Chem. Int. Ed. Engl.* **35**, 1068 (1996) and references therein. Methane complexes are now generally accepted intermediates in C–H activation reactions. To date, extensive indirect data have been obtained to support the intermediacy of such species. However, none have been isolated and characterized.
21. No H/D exchange is observed between D_2SO_4 and the methyl C–H bonds of methyl bisulate when a solution of CH_3OSO_3H (0.2 M) containing 50 mM (bpym)$PtCl_2$ is heated to 220°C for 2 hours. However, a slow rate of oxidation of methyl bisulfate to CO_2 is observed and can be considered to be a limiting rate of H/D exchange of methyl bisulfate (if we assume that all C–H activation events of methyl bisulfate lead to rapid CO_2 formation). In this case, we can estimate that the rate C–H activation of methane is at least 100 times greater than that of methyl bisulfate (*13*). No methane formation is observed in these reactions indicating that the oxidation of methane to methyl bisulfate occurs irreversible as expected.
22. Similar scrambling had been observed by Shilov (*3*) who proposed a carbene-hydride intermediate to explain the results.
23. Catalytica Advanced Technologies Inc., a wholly owned subsidiary of Catalytica Inc., acknowledges participation in this program by Syntroleum Corp.; Techmocisco Inc., a wholly owned subsidiary of Mitsubishi Oil Co., Ltd.; Petro-Canada; and the U.S. Department of Commerce, National Institutes of Standards and Technology.

23 January 1998; accepted 25 March 1998

The Lost Colony and Jamestown Droughts

David W. Stahle,* Malcolm K. Cleaveland, Dennis B. Blanton, Matthew D. Therrell, David A. Gay

Tree-ring data from Virginia indicate that the Lost Colony of Roanoke Island disappeared during the most extreme drought in 800 years (1587–1589) and that the alarming mortality and the near abandonment of Jamestown Colony occurred during the driest 7-year episode in 770 years (1606–1612). These extraordinary droughts can now be implicated in the fate of the Lost Colony and in the appalling death rate during the early occupations at Jamestown, the first permanent English settlement in America.

The network of moisture-sensitive tree-ring chronologies now available for the United States has recently been used to reconstruct summer drought and wetness on a continent-wide basis from 1700 to 1978 A.D. (*1*). Much longer chronologies are available for some areas, including a network of 800-year-long baldcypress (*Taxodium distichum*) chronologies for the southeastern United States. These exactly dated tree-ring proxies of growing-season climate can provide unique information on environmental conditions during the early colonial history of the eastern United States. Here, we use two long baldcypress chronologies to reconstruct the Palmer hydrological drought index (PHDI) (*2*) for the Tidewater region of southeastern Virginia and northeastern North Carolina (Fig. 1) and show that extreme drought afflicted the first English attempts to colonize the New World at Roanoke and Jamestown Island.

Centuries-old baldcypress trees survive locally along the Blackwater and Nottoway rivers in southeastern Virginia (Fig. 1), and exactly dated tree-ring chronologies were developed nondestructively for each location (*3*). Both chronologies are directly correlated with precipitation and are inversely correlated with temperature during the growing season (April to July), in spite of the frequently flooded riparian habitat of the sample trees (*4*). A regional baldcypress tree-ring chronology was computed as the arithmetic mean of the Blackwater and Nottoway rivers' chronologies for the common period 1185 to 1984 A.D. (variance trend due to low sample size in the early years was removed). The regional chronology is well replicated (>26 cores from 12 trees after 1225, and 62 cores at 1600) and was used to reconstruct regionally averaged July PHDI for the Tidewater and eastern Piedmont climatic divisions of Virginia and the northern and central coastal plain divisions of North Carolina (*5*). This large homogeneous climatic province includes Jamestown, Roanoke Island, and most of the drainage basins of the Blackwater and Nottoway rivers. The PHDI is closely related to the Palmer drought severity index, and both are used by the National Weather Service to monitor drought and wetness conditions across the United States (*6*). The July PHDI integrates the effects of spring and summer precipitation and temperature anomalies on the soil water balance (*2*) and is an excellent measure of

D. W. Stahle, M. K. Cleaveland, M. D. Therrell, D. A. Gay, Tree-Ring Laboratory, Department of Geography, University of Arkansas, Fayetteville, AR 72701, USA.
D. B. Blanton, Center for Archaeological Research, The College of William and Mary, Williamsburg, VA 23187–8795, USA.

*To whom correspondence should be addressed. E-mail: dstahle@comp.uark.edu

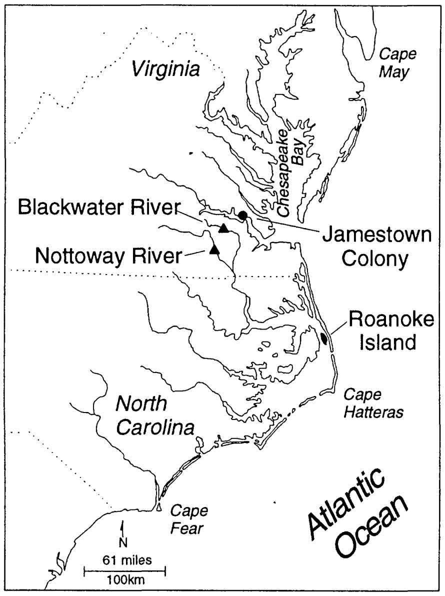

Fig. 1. Location of Roanoke Island, Jamestown Colony, and the baldcypress tree-ring chronologies from Blackwater and Nottoway rivers used to reconstruct July PHDI for the Tidewater region of Virginia and North Carolina [map adapted from (*13*)].

Table 1. Calibration and validation statistics (*3*) for the tree-ring reconstruction of July PHDI over southeastern Virginia and northeastern North Carolina [a first-differenced version (1st diff) of the reconstruction is also validated]. All results are statistically significant except the means test, where a significant difference between the observed and reconstructed means is not desirable. R^2adj. = adjusted for loss of degrees of freedom; NS = not significant.

	Calibration 1941–1984	Validation 1896–1940	Validation 1896–1940 (1st diff)
Variance explained (R^2adj.)	0.44	0.31	0.39
Pearson correlation	0.67*	0.56*	0.62*
Spearman correlation	0.67*	0.54*	0.59*
Means test (t)		1.46 (NS)	0.13 (NS)
Cross product t test	1.60*	0.84†	3.44*
Sign test (hit/miss)	32/12‡	33/12‡	29/15†
Reduction of error	0.45	0.23	0.38
Coefficient of efficiency	0.45	0.21	0.38

*$P < 0.0001$. †$P < 0.05$. ‡$P < 0.01$.

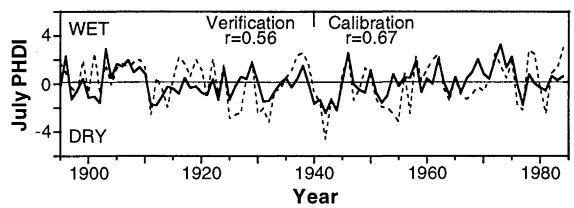

Fig. 2. Time series of the instrumental (dashed line) (*5*) and tree-ring–reconstructed July PHDI (solid line) from 1896 to 1984 for the Tidewater region.

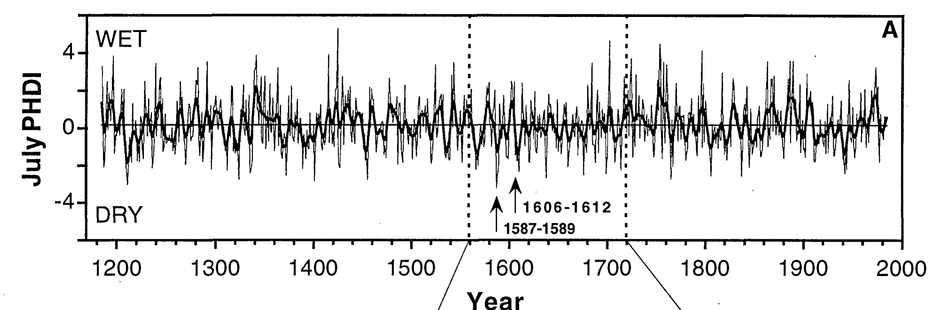

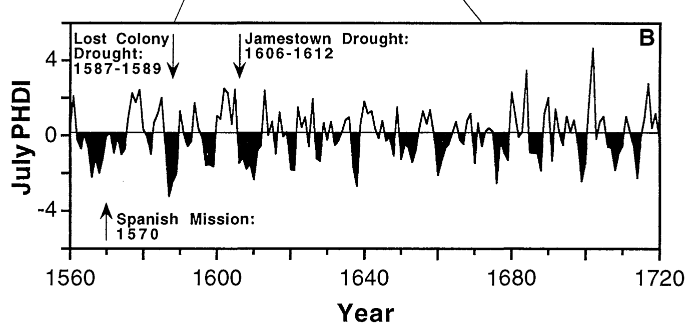

Fig. 3. Tree-ring–reconstructed July PHDI for the Tidewater region of Virginia and North Carolina from 1185 to 1984 (**A**) and for the early colonial period from 1560 to 1720 (**B**). The most extreme growing-season drought of the past 800 years was reconstructed for 1587, the year the colonists on Roanoke Island disappeared. The Lost Colony drought of 1587–1589 was the most extreme 3-year episode in the entire 800-year reconstruction. The prolonged Jamestown drought lasted from 1606 to 1612 and was the worst 7-year drought reconstructed for 770 years (from 1215 to 1984).

moisture availability throughout the growing season.

To calibrate the tree-ring and July PHDI data, the regional PHDI were first prewhitened with autoregressive (AR) modeling (*7*). July PHDI was modeled as an AR-1 process, with an AR-1 coefficient of 0.285. Regression was then used to estimate prewhitened July PHDI (y_t) from the prewhitened regional tree-ring chronology (x_t), each in year t:

$$y_t = -0.198 + 4.573x_t \qquad (1)$$

This model was developed for the period 1941–1984 and explains 44% of the variance in the instrumental July PHDI (Table 1 and Fig. 2). The AR coefficient of the instrumental July PHDI was then used to add the observed persistence structure back into the July PHDI estimates derived from Eq. 1. Estimated July PHDI (y_t) was compared with instrumental July PHDI available from 1896–1940 to validate the transfer function (Fig. 2). The suite of statistical tests for the 45-year verification period indicate that the tree-ring reconstruction provides a reasonable approximation of actual conditions, especially the first-differenced interannual fluctuations of July PHDI (Table 1).

Early Spanish references to Virginia climate further validate the accuracy of this tree-ring reconstruction at the opening of the colonial period. In September 1570 Father Juan Batista de Segura wrote that the Chesapeake Bay region had experienced 6 years of maize and wild-fruit shortages, famine, death, and parched soil (*8*). This is consistent with the reconstruction of July PHDI, which indicates a prolonged drought from 1562 to 1571 that was most severe from 1565 to 1569 (Fig. 3). Segura's commentary also documents the sensitivity of the native Algonquian subsistence system to prolonged drought, which we estimate recurred with equal or greater severity during the English settlement of Roanoke and Jamestown.

The full reconstruction of July PHDI extending from 1185 to 1984 A.D. (Fig. 3A) indicates that substantial interannual and decadal variance of growing-season moisture supply has been typical of the Tidewater region for at least the past 800 years. However, the tree-ring data specifically indicate that extraordinary drought conditions attended the settlement of both the Roanoke and Jamestown Colonies (Fig. 3). The Roanoke colonists were last seen by their English associates on 22 August 1587, the summer when the tree-ring data indicate the most extreme growing-season drought in 800 years (Fig. 3A). This drought persisted for 3 years, from 1587 to 1589, and is the driest 3-year episode in the entire 800-year reconstruction (Fig. 3). The tree growth anomaly map for the period 1587–1589 (Fig. 4A) indicates that the Lost Colony drought affected the entire southeastern United States but was particularly severe in the Tidewater region near Roanoke.

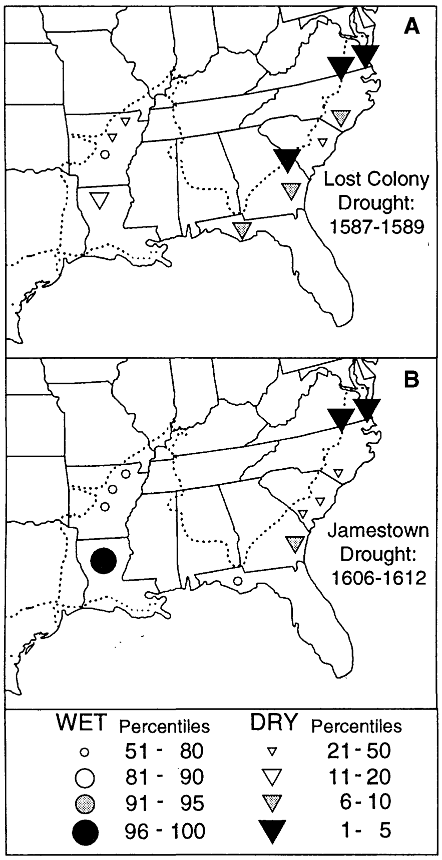

Fig. 4. Spatial pattern of growing-season drought and wetness inferred from baldcypress tree growth in the southeastern United States during the Lost Colony drought of 1587–1589 (**A**) and the 7-year Jamestown drought of 1606–1612 (**B**). Eleven drought-sensitive baldcypress chronologies were restricted to the 1185–1984 common period and were used to compute all possible 3- and 7-year consecutive averages. The percentile ranking of the 1587–1589 and 1606–1612 periods at each location is mapped. The natural distribution of baldcypress is also shown (dotted line).

The tree-ring reconstruction also indicates that the settlers of Jamestown Colony had the monumental bad luck to arrive in April 1607, during the driest 7-year period in 770 years (Fig. 3). The cypress growth anomaly map for the Jamestown drought (1606–1612) indicates that the most severe inferred drought conditions occurred in the Tidewater region near Jamestown and that above-average growth (inferred wetness) was recorded in the Mississippi Valley (Fig. 4B). This synoptic pattern is not unprecedented. A reasonable analogy can be drawn to the summer of 1993, when heavy precipitation brought record flooding to the Midwest, and severe drought occurred simultaneously over the southeastern United States (*9*).

The tree-ring data raise many interesting questions about early colonial history, beginning with the fate of the Lost Colony. Extreme drought should now be considered among the several factors responsible for the failure of the Roanoke Colony (*10–13*). Certainly, the native Croatan were concerned about the poor condition of their crops in 1587 (*13*), and the tragic shooting of friendly Croatan by the Roanoke colonists was a case of mistaken identity that arose in part from the Croatan need for food (*11*). The Lost Colony drought persisted for 3 years, and the Segura commentary (*8*) indicates that it would have created a major subsistence crisis for the native inhabitants. The Lost Colonists were dependent to a great degree on these native societies, and their dependence would have aggravated any food shortages.

Did drought contribute to the alarming mortality and near abandonment at Jamestown Colony? Only 38 of the 104 original settlers were still alive after the first year at Jamestown, and 4800 of the 6000 settlers sent to Jamestown between 1607 and 1625 died during this extraordinary period (*10, 11*). Malnutrition was a leading cause of death at Jamestown (*10*). In fact, mortality estimates for Jamestown Colony from 1608 to 1624 (*14*) as well as for the first year at Roanoke Island are significantly correlated with the tree-ring reconstructed July PHDI (Fig. 5) [1585–1586 is reconstructed as moist and only 4 of 108 people perished at Roanoke (*10*)]. The colonists were expected to live off the land and off trade and tribute from the Indians (*11*). But this subsistence system would have left the colonists extremely vulnerable during drought. Archival sources indicate that the native Algonquian people and the English domestic livestock also suffered during the years of heavy mortality among the colonists (*10*).

Poor water quality is another factor implicated in the ill health suffered at Jamestown (*14, 15*), and water quality is poorest during drought (*16*). The lower James River is a brackish estuary, and there are archival references to foul drinking water and associated illnesses among the settlers, particularly before 1613 (*14*). Reduced freshwater discharge during regional drought is associated with increased concentration of salt in the lower James River and in shallow aquifers in the vicinity of Jamestown (*16*).

The Roanoke and Jamestown colonists have been criticized for poor planning, poor support, and a startling indifference to their own subsistence (*10–13*). But the tree-ring reconstruction indicates that even the best planned and supported colony would have been supremely challenged by the climatic conditions of 1587–1589 and 1606–1612.

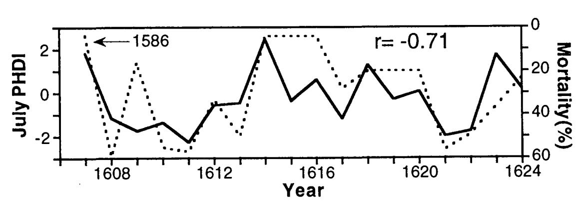

Fig. 5. Percent mortality estimates (dotted line) for Jamestown Colony (1608–1624) (*14*) and for Roanoke Colony (1585–1586) (*10*) are significantly correlated with reconstructed July PHDI (Pearson's $r = -0.71$, $P < 0.001$; Spearman's $r = -0.69$, $P < 0.002$). Mortality was summarized each spring from estimates of population and immigration (*14*), so the mortality data for 1607–1608 are compared here with July PHDI for 1607. Mortality estimates for 1614–1616 and 1618–1620 are 3-year averages.

REFERENCES AND NOTES

1. E. R. Cook, D. M. Meko, C. W. Stockton, *J. Climate* **10**, 1343 (1997); E. R. Cook, D. M. Meko, D. W. Stahle, M. K. Cleaveland, *ibid.*, in press.
2. W. C. Palmer, *U.S. Department of Commerce Weather Bur. Res. Pap.* 45 (1965).
3. M. A. Stokes and T. L. Smiley, *Introduction to Tree-Ring Dating* (Univ. of Arizona Press, Tucson, 1996); E. R. Cook and K. Kariutskis, *Methods of Dendrochronology* (Springer-Verlag, New York, 1990).
4. D. W. Stahle, M. K. Cleaveland, J. G. Hehr, *Science* **240**, 1517 (1988); D. W. Stahle and M. K. Cleaveland, *Bull. Am. Meteorol. Soc.* **73**, 1947 (1992).
5. T. R. Karl, L. K. Metcalf, M. L. Nicodemus, R. G. Quayle, *Historical Climatology Series, North Carolina and Virginia* (National Climatic Data Center, Asheville, NC, 1983).
6. American Meteorological Society, *Bull. Am. Meteorol. Soc.* **78**, 848 (1997).
7. G. E. P. Box and G. Jenkins, *Time Series Analysis, Forecasting and Control* (Holden-Day, San Francisco, 1976).
8. C. Lewis and A. Loomie, *The Spanish Jesuit Mission in Virginia, 1570–1572* (Univ. of North Carolina Press, Chapel Hill, 1953).
9. Climate Analysis Center, *Climatic Data for 1993* (Climate Analysis Center, Washington, DC, 1994), p. 67.
10. K.O. Kupperman, *J. Am. History* **66**, 24 (1979); *Settling with the Indians* (Rowman & Littlefield, Totowa, NJ, 1980); *Roanoke, the Abandoned Colony* (Row-

man & Allanheld, Totowa, NJ, 1984).
11. E. S. Morgan, *American Slavery, American Freedom, the Ordeal of Colonial Virginia* (Norton, New York, 1975).
12. D. B. Quinn, *Set Fair for Roanoke* (Univ. of North Carolina Press, Chapel Hill, 1985).
13. D. Stick, *Roanoke Island, The Beginnings of English America* (Univ. of North Carolina Press, Chapel Hill, 1983).
14. C. Earle, in *The Chesapeake in the Seventeenth Century: Essays on Anglo-American Society*, T. W. Tate and D. L. Ammerman, Eds. (Univ. of North Carolina Press, Chapel Hill, 1979), pp. 96–125.
15. I. N. Hume, *The Virginia Adventure* (Knopf, New York, 1994), p. 132.
16. B. J. Prugh, P. E. Herman, D. L. Belval, *Water-Data Report VA-91-1* (U.S. Geological Survey, Richmond, VA, 1992).
17. We thank G. M. Williamson, T. P. Harlan, and J. Young; the landowners B. Phillips and J. F. Johnson III; and the Kirk Lumber Company for assisting the protection of the ancient baldcypress trees on the Pompeii Tract at Blackwater River. Supported by the National Science Foundation, Paleoclimatology Program (grant ATM-9528148), and The College of William and Mary, Williamsburg, VA, with support from the National Park Service. The observed and reconstructed July PHDI may be obtained from the National Geophysical Data Center at ftp://ftp.ngdc.noaa.gov/paleo/treering/reconstructions/jamestown-roanoke/

27 January 1998; accepted 5 March 1998

Tunneling into a Single Magnetic Atom: Spectroscopic Evidence of the Kondo Resonance

V. Madhavan, W. Chen, T. Jamneala, M. F. Crommie, N. S. Wingreen

The Kondo effect arises from the quantum mechanical interplay between the electrons of a host metal and a magnetic impurity and is predicted to result in local charge and spin variations around the magnetic impurity. A cryogenic scanning tunneling microscope was used to spatially resolve the electronic properties of individual magnetic atoms displaying the Kondo effect. Spectroscopic measurements performed on individual cobalt atoms on the surface of gold show an energetically narrow feature that is identified as the Kondo resonance—the predicted response of a Kondo impurity. Unexpected structure in the Kondo resonance is shown to arise from quantum mechanical interference between the *d* orbital and conduction electron channels for an electron tunneling into a magnetic atom in a metallic host.

The smallest magnetic structure in condensed matter physics is a single magnetic atom in a nonmagnetic host, often referred to as a Kondo impurity. The spin of a Kondo impurity interacts with the spin of surrounding conduction electrons, leading to anomalous transport properties in dilute magnetic alloys (the Kondo effect) (*1*). For temperatures below a characteristic Kondo temperature (T_K), this interaction causes the electrons of the host metal to condense into a many-body ground state that collectively screens the local spin of the Kondo impurity (*2*). This screening cloud exhibits a dense set of low-energy excitations called the Kondo resonance that strongly influence Kondo systems (*2, 3*). Hallmarks of the Kondo effect are the disappearance of the Kondo resonance at temperatures above T_K, and the splitting of the resonance in an applied magnetic field (*2*). Although this theoretical picture has developed over more than 30 years and explains a wealth of data on magnetic alloys and rare earth compounds (*2, 4*), there remains a surprising lack of direct experimental confirmation of the theory. For example, to date there has been no direct spectroscopic observation of the Kondo resonance for an isolated, well-characterized magnetic impurity in a nonmagnetic host (*5*), nor have there been conclusive measurements of the size of the Kondo screening cloud (*6–8*).

V. Madhavan, W. Chen, T. Jamneala, M. F. Crommie, Department of Physics, Boston University, 590 Commonwealth Avenue, Boston, MA 02215, USA.
N. S. Wingreen, NEC Research Institute, 4 Independence Way, Princeton, NJ 08540, USA.

We report measurements of the local electronic structure of an isolated Kondo impurity on a metallic substrate. We used a scanning tunneling microscope (STM) to obtain spectroscopic data on individual cobalt (Co) atoms deposited onto the (111) face of a clean gold (Au) crystal at 4 K. These measurements reveal an electronic resonance centered about the Fermi energy (E_F) that has an energy width of only 11 meV and is localized to within a radius of 10 Å from the center of a Co atom. Because Co-Au is a known Kondo system (*3, 9–11*), we interpret these data as evidence of the Kondo resonance for a single, well-characterized magnetic impurity. The line shape of the observed Kondo resonance is not Lorentzian, but rather has the asymmetric shape that is characteristic of a Fano resonance (*12*). We can explain this line shape by generalizing Fano's formalism to include tunneling into an impurity with strong Coulomb repulsion. Asymmetry in the Kondo resonance line shape is thus understood to result from quantum interference between the *d* orbital and continuum tunneling channels of the magnetic atom.

Cobalt in bulk Au has a high Kondo temperature (300 to 700 K) (*3, 9, 10*), and there is evidence that Co atoms are magnetic on Au surfaces with $T_K = 19$ K (*11*). At 4 K the collective Kondo ground state is thus formed ($T < T_K$). We cleaned the single crystal Au(111) substrate in ultrahigh vacuum (UHV) by repeated cycles of Ar ion sputtering and annealing. The Au(111) surface was then cooled to 4 K and dosed in UHV with a calibrated Co evaporator. Imaging and spectroscopy were performed with a homemade UHV STM held at the same temperature as the Au sample (4 K). The convention used here is that the bias across the STM tunnel junction (V) is the voltage of the sample with respect to the tip.

A 400 Å by 400 Å image of the Au(111) surface after deposition of a 0.001 monolayer coverage of Co (Fig. 1) shows the well-known Au(111) herringbone reconstruction (*13*), seen as ridges (or "soliton walls") traversing the surface. The soliton walls separate regions of face-centered cubic (fcc) and hexagonal close-packed (hcp) ordering on the surface (*13*). Approximately 22 well-isolated Co atoms can be seen as regular 0.8 Å high cones scattered about the surface (some surface defects can also be seen). Closer examination shows that the Au sur-

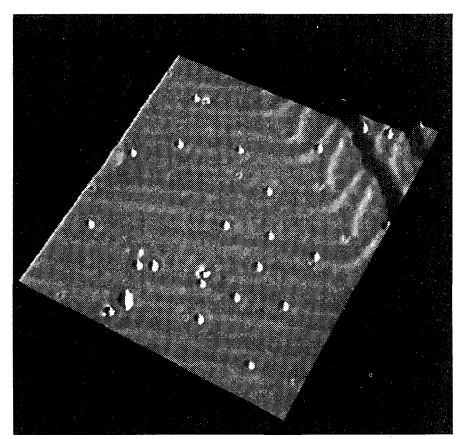

Fig. 1. Constant-current image (400 Å by 400 Å) of the Au(111) surface after deposition of 0.001 monolayer of Co at 4 K (tunnel parameters: $I = 0.5$ nA, $V = 0.1$ V). Approximately 22 Co atoms can be seen nestled among the ridges of the Au(111) herringbone reconstruction.